

## PETROPHYSICAL CHARACTERISTICS OF THE LOWER SAFA MEMBER IN QASR FILED NORTH WESTERN DESERT, EGYPT

M. ABU-HASHISH<sup>(1)</sup>, H. ELSHAYEB<sup>(1)</sup>, A.E. FARAG<sup>(2)</sup> and H. HANE<sup>(3)</sup>

(1) Geology Department, Menoufiya University, Egypt, (2) British University,  
Cairo, Egypt and (3) Schlumberger Company.

(3) Email: haneharby@gmail.com

### تقييم الخزان لعنصر صفا السفلى فى حقل قصر فى الشمال الشرقى ، الصحراء الغربية ، مصر

**الخلاصة:** يعتبر الحقل موضع الدراسة من أكبر الحقول المنتجة فى الصحراء الغربية الذي يتكون من حجر رملي مع تداخلات من الحجر الطفلي بناء على البيانات المتوفرة والممثلة في التسجيلات الجيولوجية وتحليل تسجيلات الآبار المتاحة لحساب الخواص البتروفيزيائية لصخور خزان صفا الممثلة في الحجر الرملي لي الآبار المتاحة وهي : قصر-4 و قصر-5 و قصر-6 و قصر-12 و قصر-15، يشمل تحليل سجلات هذه الآبار تحديد الخواص البتروفيزيائية لصخور الخزان في حجم المحتوى الطفلي والمسامية الكلية والفعالة والتشبع بالسوائل وسمك الخزان الصافي لتعكس الإختلاف الراسي والأفقى فى الخصائص البتروفيزيائية للخزان من خلال خرائط التوزيع التي تم بناؤها لمنطقه الدراسة. وقد نتج عن ذلك ان لدي عضة صفا خصائص بتروفيزيائية جيدة مما يجعله خزانا جيدا يتميز بمتوسط حجم المحتوى الطفلي يتراوح بين 3% إلى 16% و المسامية الفعالة من 11% إلى 16% التشبع بالماء من 5% إلى 29% وتشبع الهيدروكربون من 95% إلى 71% تم استخدام طريقة توماس ستير لتحديد نوع طبقة للطفله الموجوده وايضا تم استخدام التصوير الدقيق للتكوين لتحديد الخواص الترسيبيه والتركيبه للخزان .

**ABSTRACT:** The Qasr Field is characterized by gas production zones . which contains sandstone interbedded with shale, based on the available data represented by geological composite logs and different types of open-hole wireline logs for five wells (QASR-4, QASR-5, QASR-6, QASR-12 and QASR-15). Reservoir distribution maps show that the reservoir net pay thickness of the Lower Safa Member ranges from 108 -390 ft, the effective porosity map shows that the reservoir porosity ranges from 11-16% , the shale content map shows that the shale content ranges from 3-16%, the water saturation map shows that the water saturation ranges from 5-29% and hydrocarbon saturation varies from 71-95%. The thin beds have been better defined and reservoir capacity has been maximized in this way by an interpreting method introduced by Thomas Stieber Method . Which enables identification in heterogeneous sandstones of clean sandstone sections. The high porosity sections and thus the good reservoirs generally represent clean sandstone. Quantifying such reservoirs can also lead to highly useful concepts. Knowledge of the sedimentary features is important for determining reservoir geometry and petrophysical reservoir parameters FMI tools was used for recognition of sedimentary and structural features in microresistivity images.

## INTRODUCTION

The Qasr Field is located in the northeastern part of Shushan basin in the northern part of the Western Desert of Egypt, bounded by latitudes 30° 35' to 30° 40' N and longitudes 26° 30' to 26° 50' E (Fig. 1). The Lower Safa Member consists of sandstone, siltstone with some shale streaks, indicating shallow marine facies, its sequence may reach a maximum thickness of over 900 feet in the northeastern part of Shushan basin (Qasr Field). Different wireline logs suites (Gamma ray, Neutron, Density, Sonic, Resistivity, etc.), for five wells namely QASR-4, QASR-5, QASR-6, QASR-12 and QASR-15 were used in the analysis and performing the necessary calculations. The most important petrophysical parameters necessary for characterizing the potential reservoirs are Shale volume, effective porosity, fluid saturations. Analysis of available well

logs includes determination of the petrophysical properties of reservoir rocks namely the shale volume (Vsh), porosity , fluid saturation (sw & Sh), and net-pay thickness to reveal the vertical and horizontal variations of reservoir characteristics through constructing the litho-saturation crossplots and iso-parametric maps of the study area.

### General Geology

The Western Desert of Egypt covers an area of approximately 700,000 km<sup>2</sup> which represents two thirds of the total area of the country (EGPC, 2009), the study area lies in the Shoushan Basin in the northern Western Desert focusing on the QASR filed, which is the most productive gas field in the Shoushan Basin (Fig. 1).

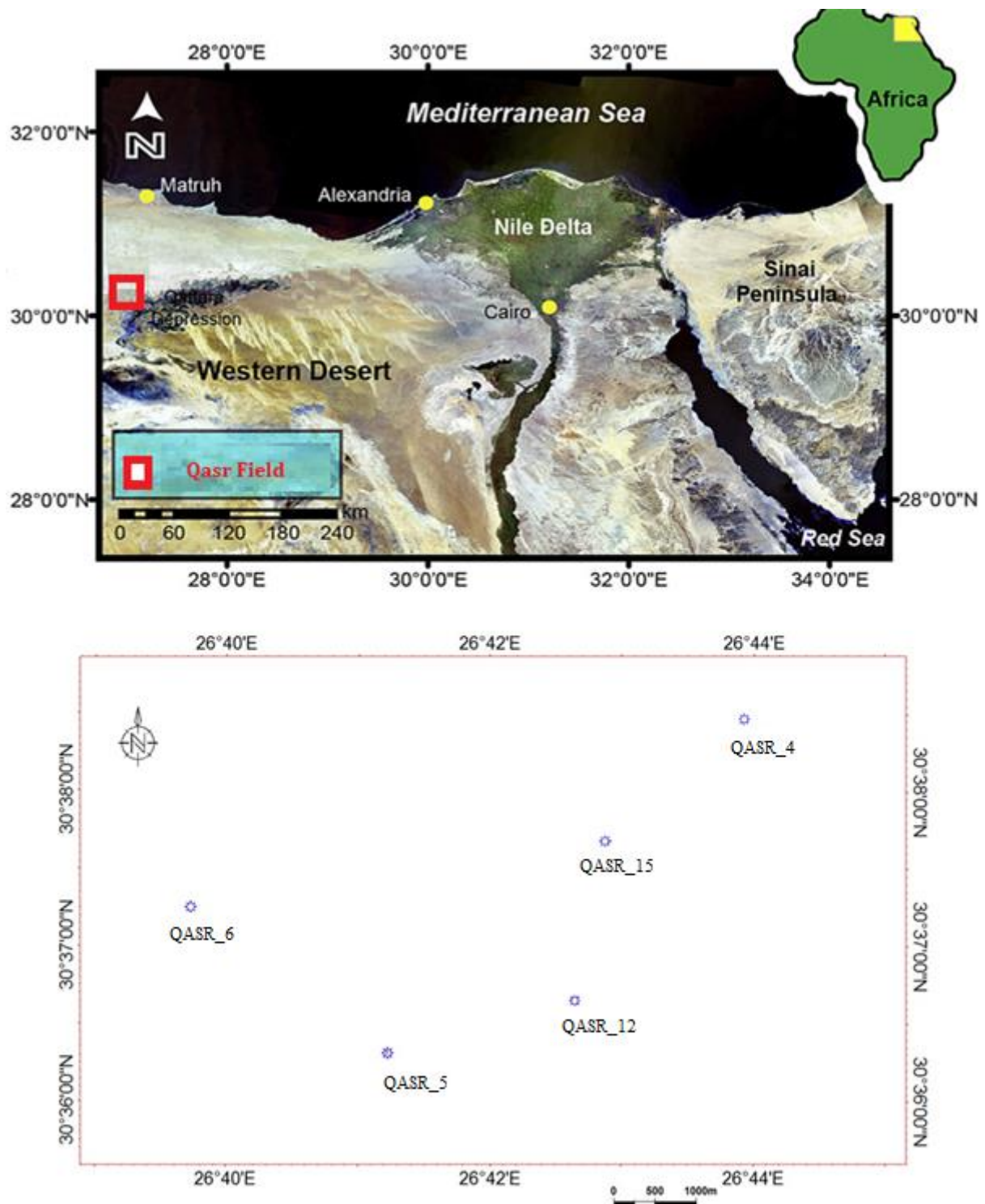


**Fig. 1:** Location map of the study area showing different basins and sub-basins within the Western Desert and spatial distribution of the studied wells in the Qasr field.

The Shoushan Basin in the northern Western Desert of Egypt still has significant hydrocarbon potential as recent oil, and gas discoveries have suggested (Dolson JC, Shann MV, Matbouly SI, Hammouda H, Rashed RM 2001). The Shoushan Basin contains sediments of Jurassic and younger ages. The hydrocarbons (oil and gas) accumulated in the Jurassic to Cretaceous formations, where source rocks are found in the Jurassic and Cretaceous successions (Fig. 2) (El Ayouty MK 1990). Sandstones of the Middle Jurassic Lower SAFA Member, Khatatba Formation contain some of the largest gas resources in the northern Western Desert region. The gas is thought to be sourced mostly from the Jurassic and Lower Cretaceous formations (Fig. 2).

**Methodology**

A full set of well logs includes Caliper (HCAL), Gamma Ray (GR), Natural gamma ray spectrometry

(NGS), Resistivity (LLS, LLD), Bulk Density Log (RHOB), Neutron Log (NPHI), and Sonic Log ( $\Delta t$ ), for five wells QASR\_4, QASR\_5, QASR\_6, QASR\_12 and QASR\_15 ), in Khalda land field was used to estimate the petrophysical properties and to evaluate the reservoir characteristics of Lower Safa Member within vertical and lateral changes of rock facies, through analyzing and interpreting the data, which are essentially analytical, based on a number of equations and empirical formula and charts recommended by Schlumberger Principles and Essentials (1972), Dresser Atlas, (1983), and Schlumberger Log Interpretation Charts (2009), to calculate and determine the formation temperature, volume of shale, total and effective porosity, water and hydrocarbon saturation, net pay thickness, that achieved by using integrated computer software Techlog (2018.2), also identify lithology and clay minerals types through a number of different constructed crossplots.

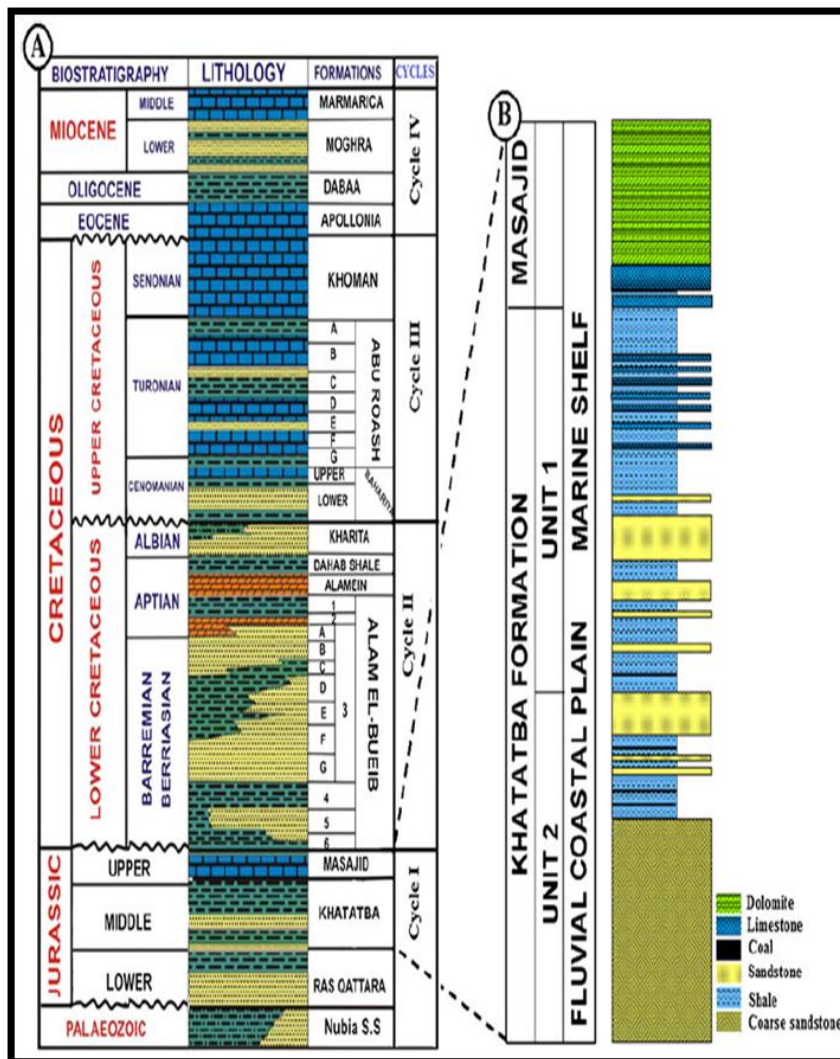


Fig. 2: Generalized stratigraphic column of the north Western Desert of Egypt (Shalaby et al., 2014).

## WELL LOG ANALYSIS

The well logging analysis deduced parameters, resulted from Computer Processed Interpretation (CPI). The process includes volume of shale, total porosity, effective porosity, water and hydrocarbon saturation and also net pay zones through the following procedures, and tabulated in table (1).

### Determination of Shale Volume (Vsh):

Estimation of shale volume was carried out using both single (Gamma Ray log) and double clay indicator (Neutron-Density combination) according to (Equations. 1 and 2).

$$I_{GR} = \frac{GR_{log} - GR_{min}}{GR_{max} - GR_{min}} = Vsh_{GR} \quad (\text{eq. 1})$$

$$Vsh_{N-D} = \left\{ \frac{\phi_N - \phi_D}{Q_{NSH} - \phi_{Dsh}} \right\} \quad (\text{eq. 2})$$

### Determination of Formation Porosity ( $\phi$ ):

The quality of a reservoir is defined by its hydrocarbon storage capacity and deliverability that can be determined through the porosity volume of reservoir rocks. The total porosity has calculated using Neutron-Density method using Equation (3), and effective porosity has been calculated from the total porosity by using Equation (4),

$$\phi_{N-D} = \sqrt{\frac{\phi_N^2 - \phi_D^2}{2}} \quad (\text{eq. 3})$$

$$\phi_E = \phi_T(1 - Vsh) \quad (\text{eq. 4})$$

### Determination of Formation Water Resistivity (Rw):

Determination of the formation water resistivity (Rw) is very vital for well log interpretation since it is essential for the calculation of fluid saturation (Serra, 1984). It characterizes a problematic petrophysical parameter because it is not constant in nature. It is determined using laboratory measurement, which have been applied to all the premeditated wells (Schlumberger, 2009). The value of formation water resistivity (Rw) for the Lower Safa Member is obtained from Core data = 0.017 ohmm, m = 1, n = 2 and a = 1.

### Determination of Fluid Saturation (Sw & SH):

Most of the reservoirs at least consist of two different phases of liquids. These phases are gas and water or oil and water. Some of the reservoirs have all of the three phases of gas, oil and water (Dandekar, 2006). The determination of the fluids saturation involves principally the discrimination between the various fluid components (water and hydrocarbons). Determination of reservoirs water saturation is vital because it refers to the saturation of hydrocarbons in the reservoir. The water saturation is predictable in both the

uninvaded-zone (Sw) and flushed zone (Sxo) using Indonesia equation; accordingly the hydrocarbon saturation has been calculated depending upon the water saturation (Schon, 2011).

### Net pay calculation:

The calculated net pay, porosity, water saturation and hydrocarbon saturation are tabulated and mapped for Lower Safa. The cutoffs used for the Lower Safa are as follows: volume of shale 35%, effective porosity 10% and water saturation 60%.

### Determination of Shale Models:

Clays are usually distributed in the formation in 3 ways:

- 1) Laminated shales: Continuous bands of shale layers interbedded with sand layers.
- 2) Dispersed shales: Clays found in pore spaces or coating sand grains.
- 3) Structural shales: Clays that are part of the formation matrix.

The Module which used is Thomas-Stieber Shaly Sand Model was originally invented to resolve the problem of laminated shaly-sand sequences, in the conventional methods, the correlation between the gamma ray parameter and the shale volume is usually presented as one direct relationship. Because the shale can exist in three different forms in the sand: dispersed, laminated and structural, the method expects a correlation between the varying gamma ray responses and the shale geometry (Thomas & Stieber, 1975).

### FMI (Formation Micro Imager) FMI Analysis:

FMI logs can be used to study the orientations of carbonate and shale beds in the well, as well as the orientations of faults and fractures in these Image logs are displayed using bright colors for resistive units, and lower resistivity conductive units are displayed using dark colors and the interpretation typically started with hand picking dips using sinusoid techniques on oriented images presented at 1:20 or 1:10 scale that the geological features are easily visualized in Borview (Geoframe). Once dips have been picked, it is classified into bed boundaries and fractures. The structural dip data are imported into the Bortex and the heterogeneity analysis of reservoirs from borehole images

### CROSS-PLOTTING

Whereas, the identification of lithology is of a particular importance in formation evaluation process, therefore, crossplot technique represents another effective method for visualizing petrophysical data, which can be used to identify lithology and clay minerals types and form. For this purpose different types of crossplots have been constructed for lithology identification as Neutron-Density, Density-PEF and Umaa – pmaa crossplot, also identifying clay minerals types and form as NGS Cross-Plot and Thomas-Stieber Plot.

**Lithological Identification Crossplots:  
Neutron-Density Crossplot:**

Identification of lithology is of a particular importance in formation evaluation process. Logs can be used as indicators of lithology. The most useful logs for this purpose are density, neutron, sonic and gamma-ray logs. Fig. 3 shows the neutron-density and the neutron-sonic crossplots (lithological identification cross plot) of Lower Safa Member of the Khatatba Formation in Qasr Field. As is shown in this figure, it is mainly characterized by the predominance of reefal limestone. It is also characterized by the presence of shale.

**Density-PEF Crossplot:**

The bulk density versus photoelectric cross section index cross-plot is useful to identify the mineral composition in a single or two mineral matrixes where the minerals are known. Density-PEF cross-plots have been constructed for 5 wells (QASR-4, 5, 6, 12 and 15). The results point out the presence of sandstone and shale as the main components of Lower Safa Member, whereas the shale points are shifted towards the dolomite (Fig. 4), and this is well matched with cutting samples descriptions of Lower Safa Member on mud log.

**Determination of Shale Minerals Type CrossPlot:**

In this sand shale and fluid system we need to define the properties of clean sand, pure shale and the fluid. This is done by plotting our data on a Thomas-Stieber cross-plot .Clean sand and pure shale points are picked graphically on the plot. On the charts below. Sand point ( $V_{sh} = 0$ ) represents a system where the matrix is 100% sand and associated porosity is  $PHI_{max}$ . Shale point ( $V_{sh} = 1$ ) represents a system with matrix and porosity filled with 100% shale and the porosity in this shale is  $PHI_{sh}$ . The effective porosity of this system is 0. Structural shale point represents a system where all the sand in the matrix is replaced by shale but the pore space is untouched ( $V_{sh} = 1 - PHI_{max}$ ). Thus the total porosity in this system is  $PHI_{max} + PHI_{sh} * (1 - PHI_{max})$  Dispersed shale point represents a system where the matrix is 100% sand but the pore space is filled with 100% shale ( $V_{sh} = PHI_{max}$ ). Thus the total porosity in this system is  $PHI_{sh} * PHI_{max}$ . The Upper Bahriya reservoir in the study area is characterized by clean sand, laminated shale and some dispersed shale. as in the figure below Fig.14 Gamma ray porosity Cross-Plot of Upper Bahariya reservoir the study area , Thomas-Stieber's plot was constructed for all available well to determine the distribution modes of shale in sand bodies, which show that dispersed types are represented within the reservoir (Fig. 5)

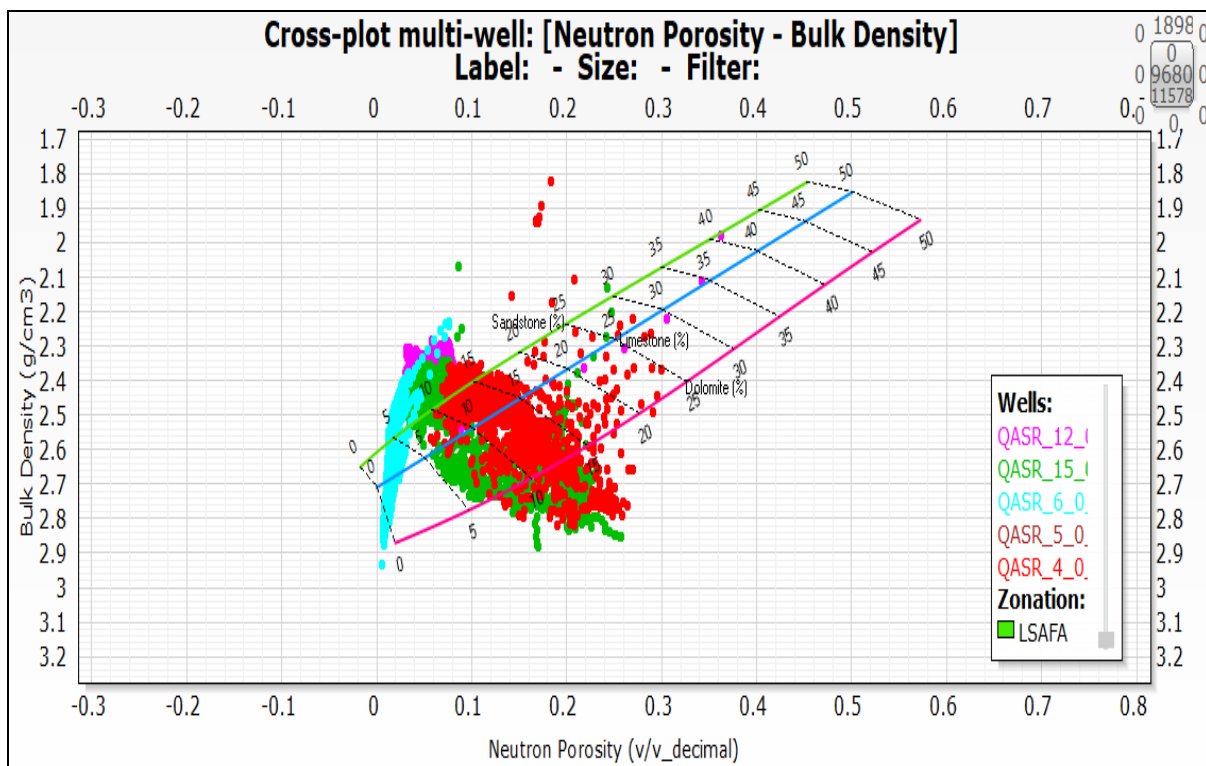


**Fig. 3: Lithological identification crossplot for the Lower Safa Member of Khatatba Formation.**

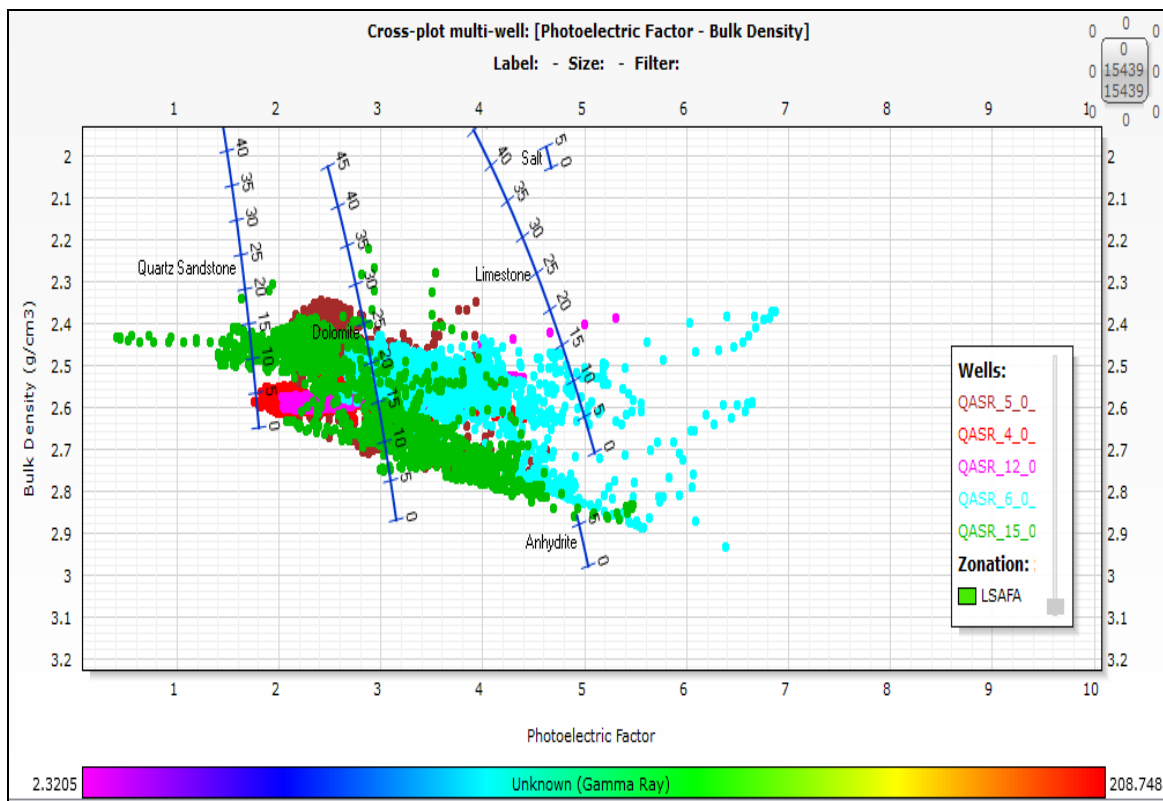


Fig. 4: Density-PEF crossplot of well for the Lower Safa Member of Khatatba Formation.

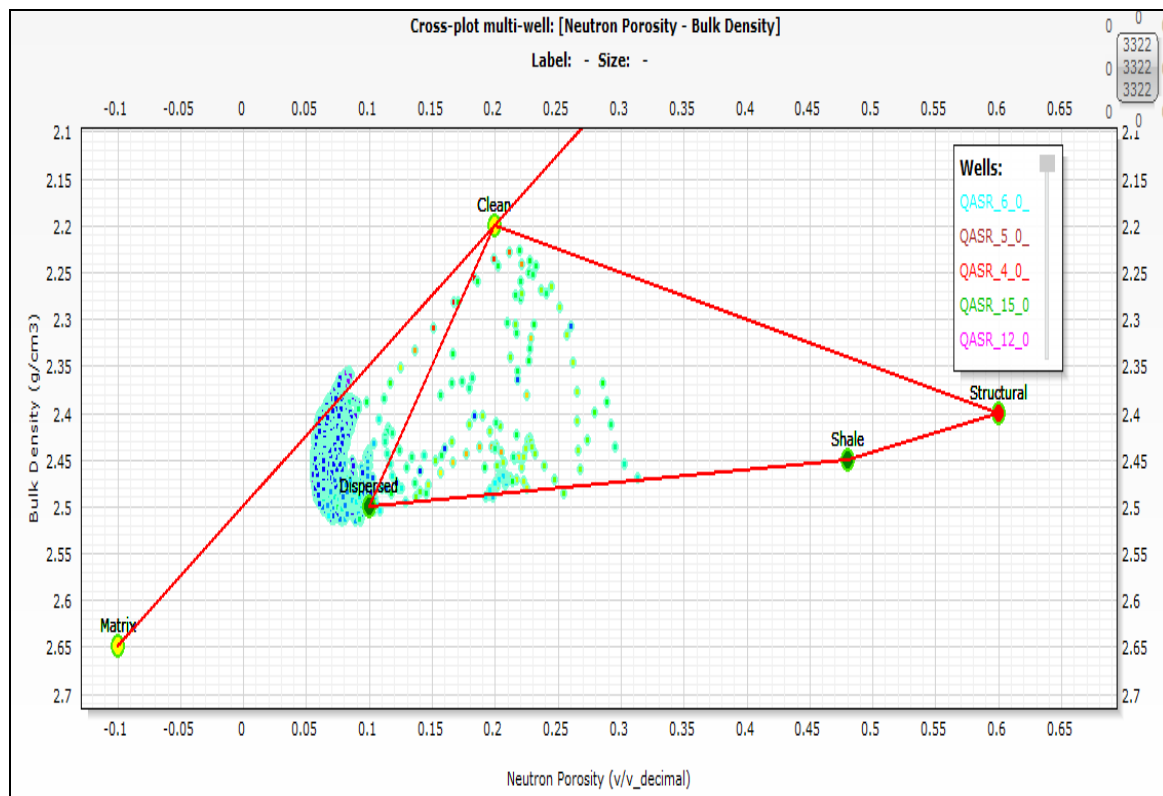


Fig. 5: Thomas-Stieber crossplot of wells (QASR-4, 5, 6, 12 and 15).

**RESERVOIR EVALUATION**

Evaluation of reservoir rocks of the Lower Safa Member using petrophysical parameters, namely shale volume, porosity (total and effective), and water and hydrocarbon saturation; and identifying the pay and nonpay zones related to the determined cutoffs of parameters, through Computer Processed Interpretation (CPI) using Techlog program are represented diagrammatically in the form of litho-saturation crossplots or iso-parametric maps showing the variations in reservoir properties in vertical and lateral extensions, respectively.

**Vertical Variation of Petrophysical parameters:**

Litho-saturation cross-plots signify one of the most vital well log interpretation processing data and reservoir estimation for explaining the gross characters of petrophysical parameters, in terms of lithology fractionations and fluid saturations through the well in the vertical direction. The Litho-saturation cross-plot Qasr field (indicating that the Lower Safa Member covers an interval ranging from 581 ft to 950 ft, It is composed mainly of sandstone intercalated with shale, with 108 ft-309 ft net-reservoir. The computer processed interpretation (CPI) of well logs in this well reflects a good pay that is characterized by average 3-16 % shale volume, 11-16 % average effective porosity and 5-28 % average water saturation. Fig. (6,7,8,9 and 10) illustrate the litho-saturation cross-plot for the Lower Safa Member in QASR-4,5,6, 12 and 15 wells. It is composed mainly of sandstone intercalated with shale, that is considered a net-pay.

**Lithosaturation cross plot of lower Safa Member of Khatatba Formation in well Qasr-6:**

Figure (6) illustrates the computer processed interpretation (C.P.I) plot of the Lower Safa Member of Khatatba Formation in well Qasr-6. As shown in this figure, the Lower Safa Member is encountered at depth from 13350 to 14050 ft. The gross interval of the Lower Safa Member is 900 ft. In this Formation, the net pay thickness in this well 390 ft, The shale content varies from 3 % and increase downwards. The average effective porosity varies from 12 % and decrease

downwards. The hydrocarbon saturation ranges between 89%, it generally decreases downwards.

**Lithosaturation cross plot of lower Safa Member of Khatatba Formation in well Qasr-5:**

Figure (7) illustrates the computer processed interpretation (C.P.I) plot of the Lower Safa Member of Khatatba Formation in well Qasr-5. As shown in this figure, the Lower Safa Member is encountered at depth ranges from 13000 to 14040 ft. The gross interval of the Lower Safa Member is 950 ft, the net pay thickness in this formation 138 ft , The shale content varies from 5 % and increase downwards. The average effective porosity varies from 12.4 % and decrease downwards. The hydrocarbon saturation ranges between 72%, it generally decreases downwards.

**Lithosaturation cross plot of lower Safa Member of Khatatba Formation in well Qasr-4:**

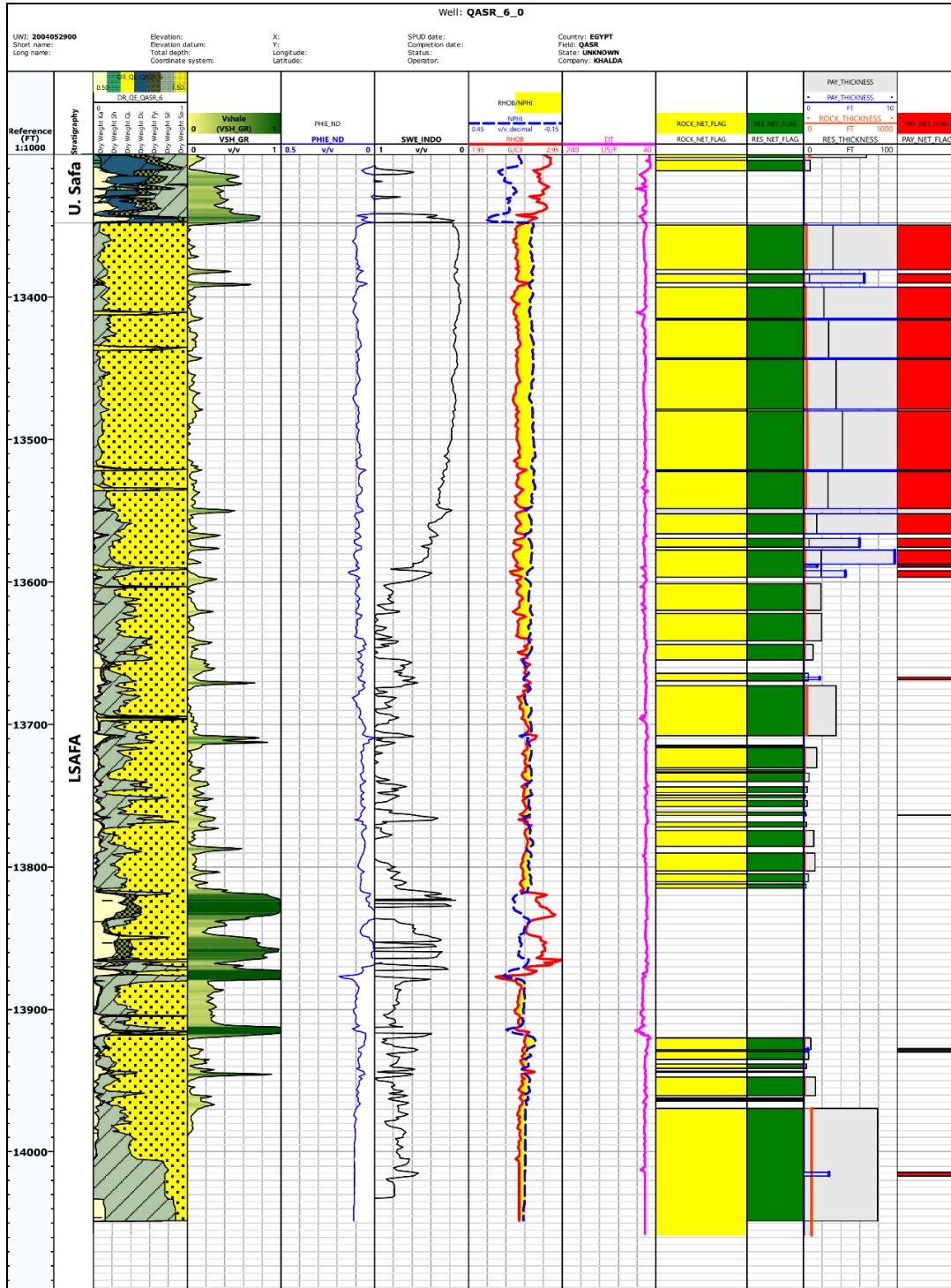
Figure (8) illustrates the computer processed interpretation (C.P.I) plot of the Lower Safa Member of Khatatba Formation in well Qasr-4. As shown in this figure the Lower Safa Member is encountered at depth from 13080 to 13900 ft. The gross interval of the Lower Safa Member is 877 ft. In this Formation, the net pay thickness in this formation 108 ft, The shale content varies from 12 % and increase downwards. The average effective porosity varies from 16.1 % and decrease downwards. The hydrocarbon saturation ranges between 71%, it generally decreases downwards

**Lithosaturation cross plot of lower Safa Member of Khatatba Formation in well Qasr-15:**

Figure (9) illustrates the computer processed interpretation (C.P.I) plot of the Lower Safa Member of Khatatba Formation in well Qasr-15. As shown in this figure the Lower Safa Member is encountered at depth from 13170 to 13740 ft. The gross interval of the Lower Safa Member is 581 ft. In this Formation, the net pay thickness in this formation 256 ft, the shale content varies from 16 % and increase downwards. The average effective porosity varies from 11.5 % and decrease downwards. The hydrocarbon saturation ranges between 79%, it generally decreases downwards.

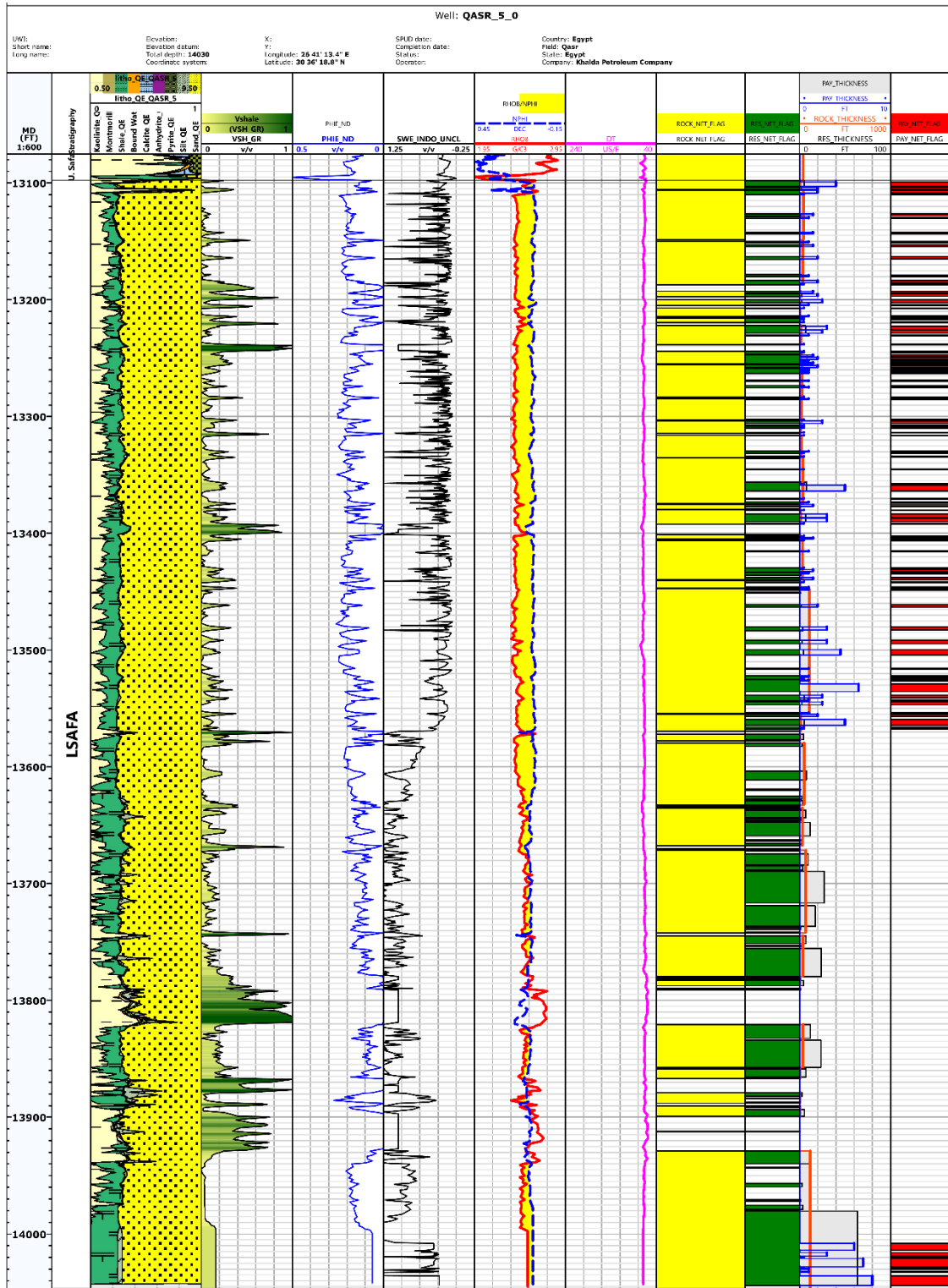
**Table (1): Summary of petrophysical parameters of Lower Safa Member in the studied wells, QASR field.**

Well No.	Shale Content (V <sub>sh</sub> %)	Effective Porosity (Φ <sub>eff</sub> %)	Water Saturation (S <sub>w</sub> %)	Gross Interval (ft.)	Hydrocarbon Saturation (S <sub>hr</sub> %)	Net Pay (ft.)
QASR-4	12	16.1	29	877	71	108
QASR -5	4	12.4	28	950	72	138
QASR -6	3	12	11	900	89	390
QASR-12	5	13	5	715	95	132
QASR-15	16	11.5	21	581	79	256



**Fig. 6: Lithosaturation Crossplot for the Lower Safa Member of Khatatba Formation in Qasr-6 Well.**





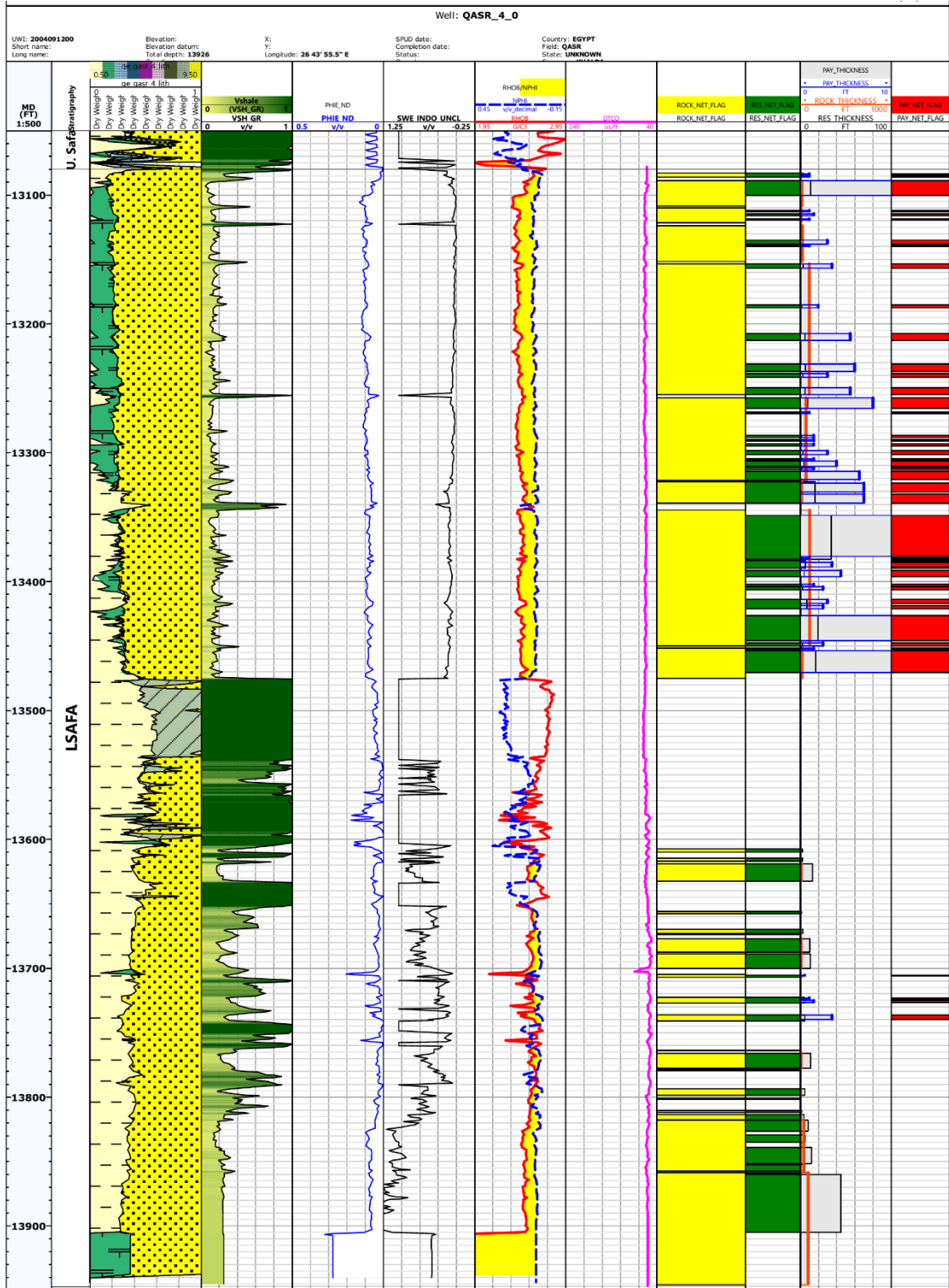


Fig. 8: Lithosaturation Crossplot for the Lower Safa Member of Khatatba Formation in Qasr-4 Well.

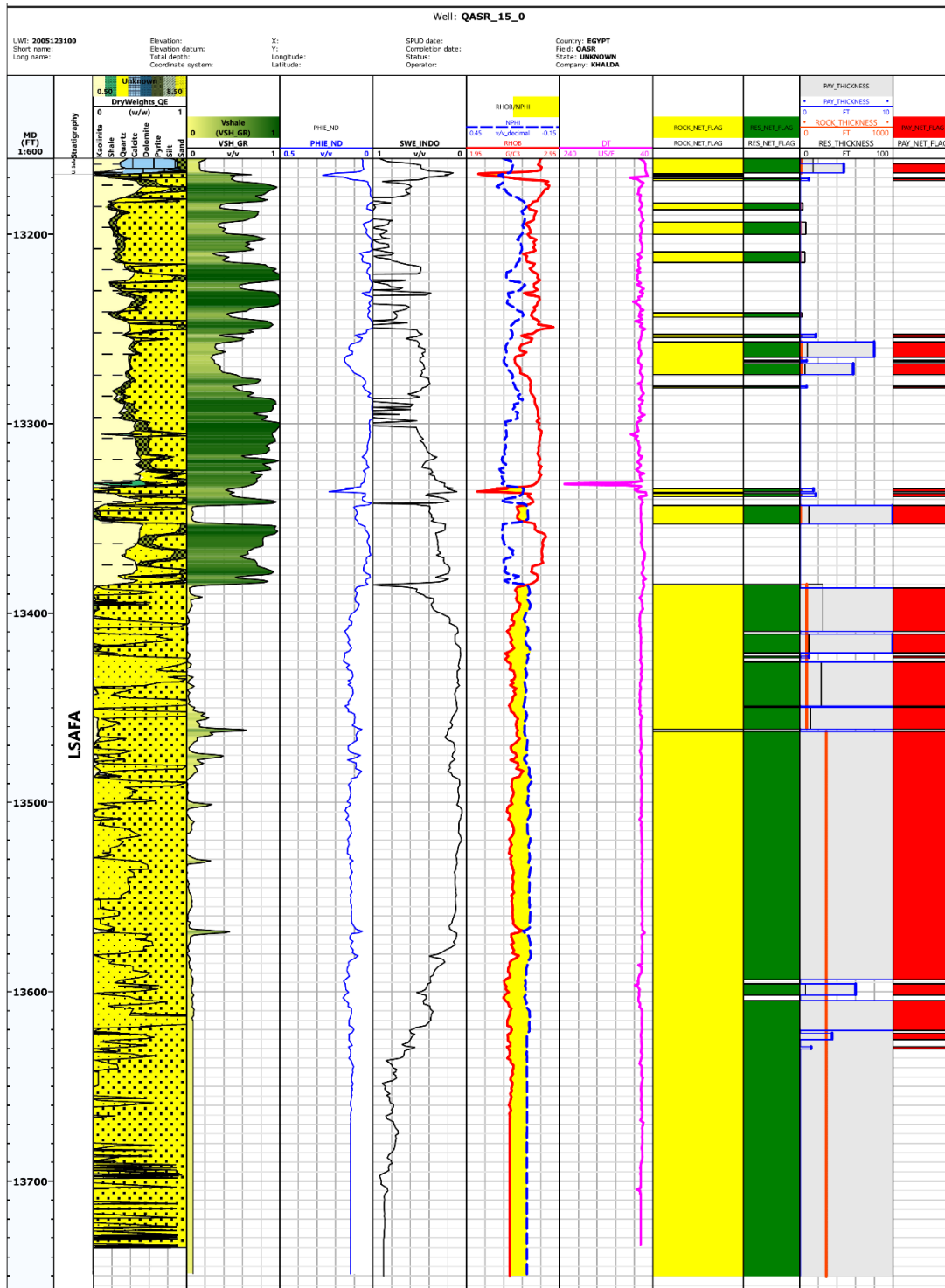
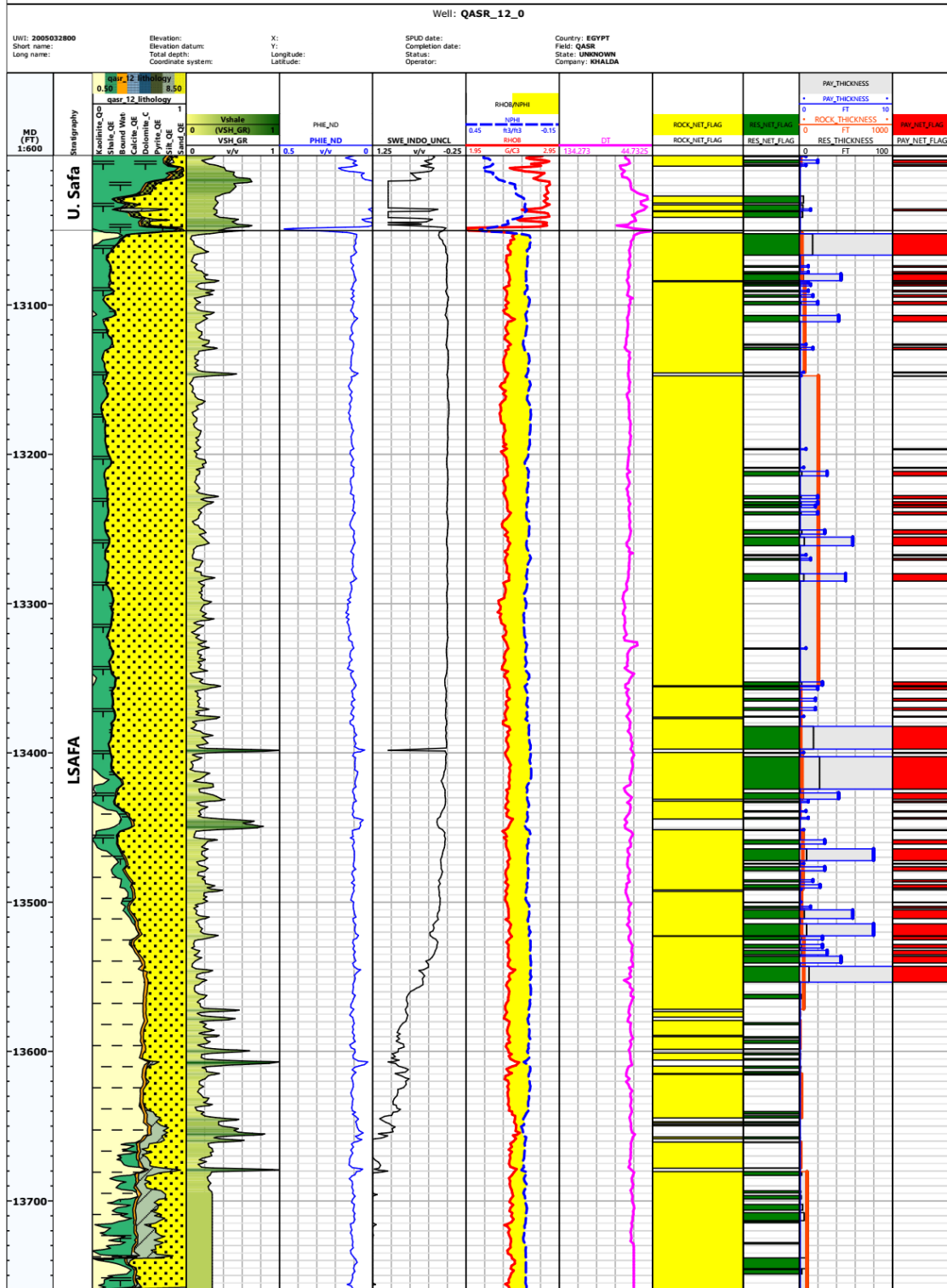


Fig. 9: Lithosaturation Crossplot for the Lower Safa Member of Khatatba Formation in Qasr-15 Well.

**Lithosaturatation Cross Plot of lower Safa Member of khatatba Formation in Qasr-12:**

Figure (10) illustrates the computer processed interpretation (C.P.I) plot of the Lower Safa Member of Khatatba Formation in well Qasr-12. As shown in this figure the Lower Safa Member is encountered at depth ranges from 13050 to 13750 ft. The gross interval of the

Lower Safa Member is 715 ft. In this Formation, the net pay thickness in this formation 132 ft, the shale content varies from 5 % and increase downwards. The average effective porosity varies from 13 % and decrease downwards. The hydrocarbon saturation ranges between 95%, it generally decreases downwards.



**Fig. 10: Lithosaturatation Crossplot for the Lower Safa Member of Khatatba Formation in Qasr-12 Well.**

**Lateral Variation of Petrophysical Characteristics:**

A number of iso-parametric maps, which are the net pay, shale content, effective porosity, water saturation, and hydrocarbon saturation maps, represent the lateral variation of petrophysical characteristics.

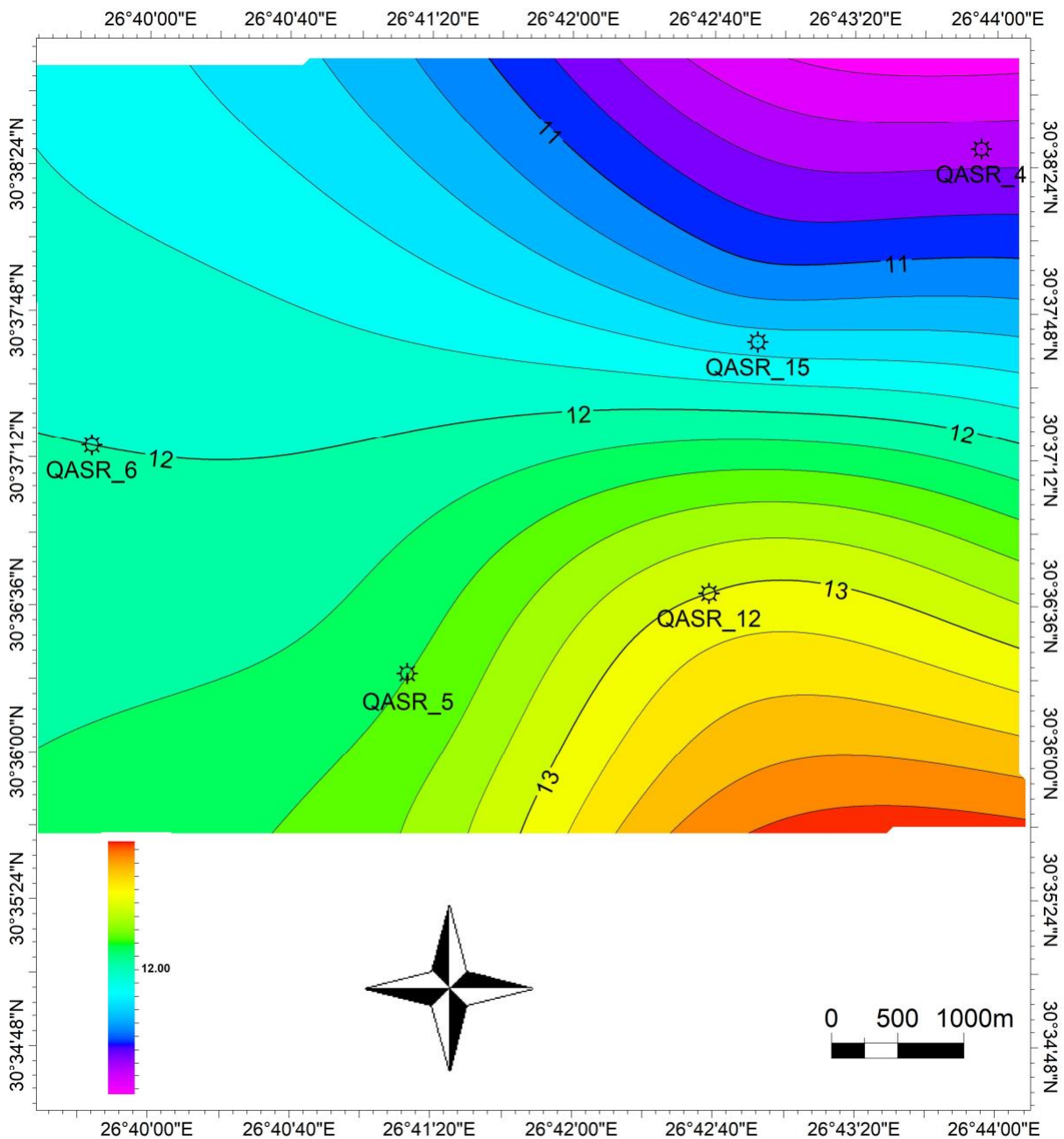
**LOWER SAFA Porosity ( $\phi_{eff}$  %) Distribution Map:**

Figure (11) shows the porosity distribution of LOWER SAFA Member. The most frequent porosity are observed within the range of 11% TO 16%. The highest value of effective porosity increases in the central and southeastern parts and decreases in the

northeastern part of the study area

**LOWER SAFA water saturation ( $S_w$  %) distribution map:**

Figure (12) shows the distribution of water saturation of LOWER SAFA in the study area. The most water saturation occurrence is observed within the range of 5% to 29% in. The highest value of water saturation increases in the south west and northeastern parts while it decreases in the central and south east parts of the study area.



**Fig. 11:** The effective porosity map for the Lower Safa. This map shows that the effective porosity increases in the central and southeastern parts and decreases in the northeastern part of the study area.

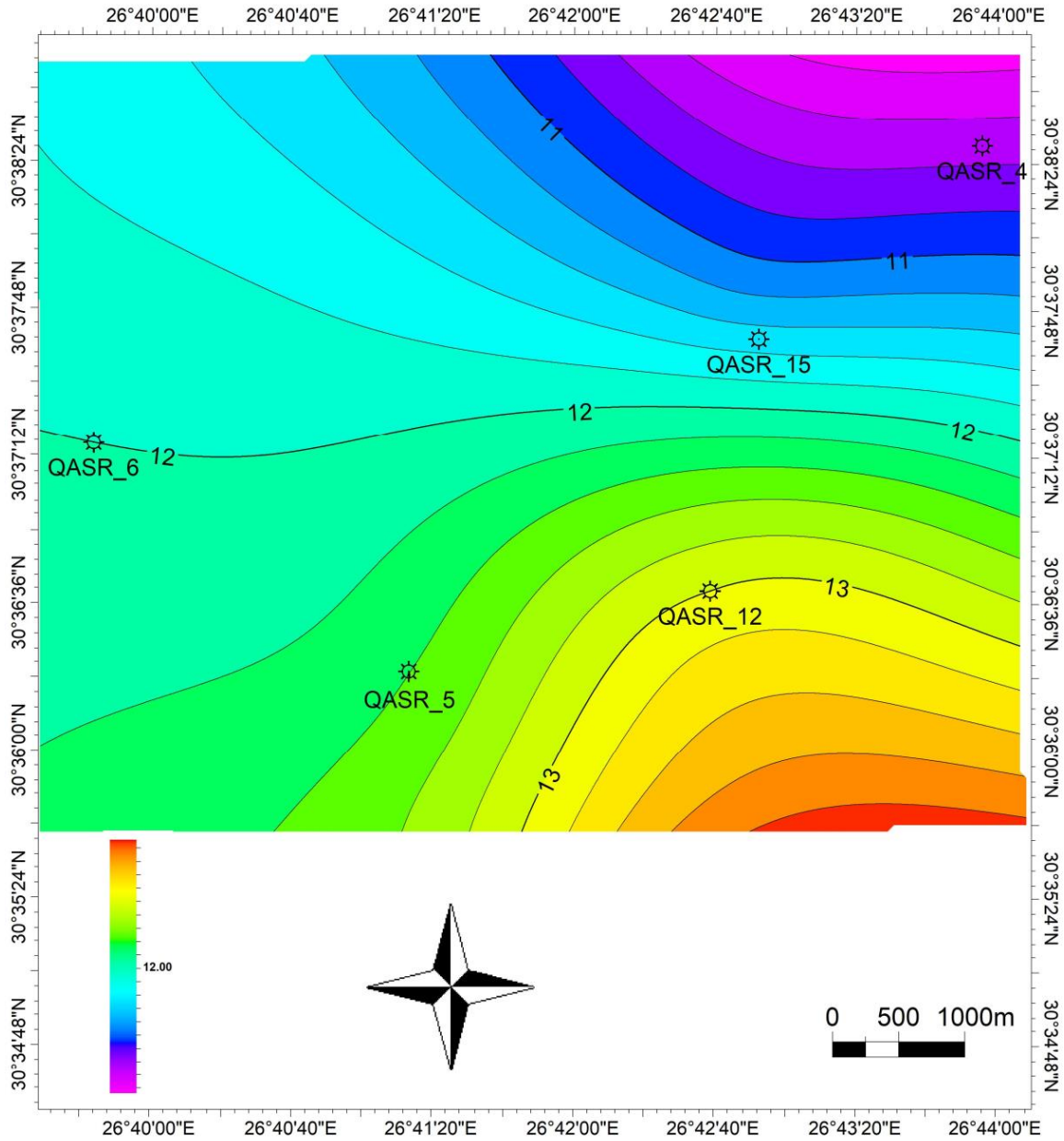


**Fig. 12: Water saturation map for the lower safa Member in the study area. This map shows that the water saturation increases in the south west and northeastern parts while it decreases in the central and south east parts of the study area.**

**Shale content (Vsh %) variation map:**

Shale content is an important quantitative function of log analysis. It is considered as an important indicator of reservoir quality, in which the lower the shale content usually reveals a better reservoir. Fig. 13 shows the distribution of shale content of Lower Safa in the study area. This map illustrates that the shale content ranges from 3% to 16 %. It increases in the north and east part and decrease gradually to the south and west part of the study area.

**Hydrocarbon saturation variation map:**

Determination of hydrocarbon saturation (Shr %) is the main target of the current study. Fig. 15 shows the hydrocarbon saturation of LOWER SAFA. This map

illustrates that the hydrocarbon saturation ranges from 71% to 95 %. This map illustrates that the hydrocarbon saturation increases in the central and northwestern parts, southeast part in the study area and decreases in the southwestern and northerneast part of the study area.

**Net pay thickness map:**

The net pay thickness distribution, the thickness ranges between 108 to 390 ft Fig. 14, shows that the highest thickness of the pay zone concentrated in the North parts of the study area and decreased in the southeastern of the study area. This map indicates that the central and northwestern parts of the study area are the most promising parts for hydrocarbon accumulations of the study area.

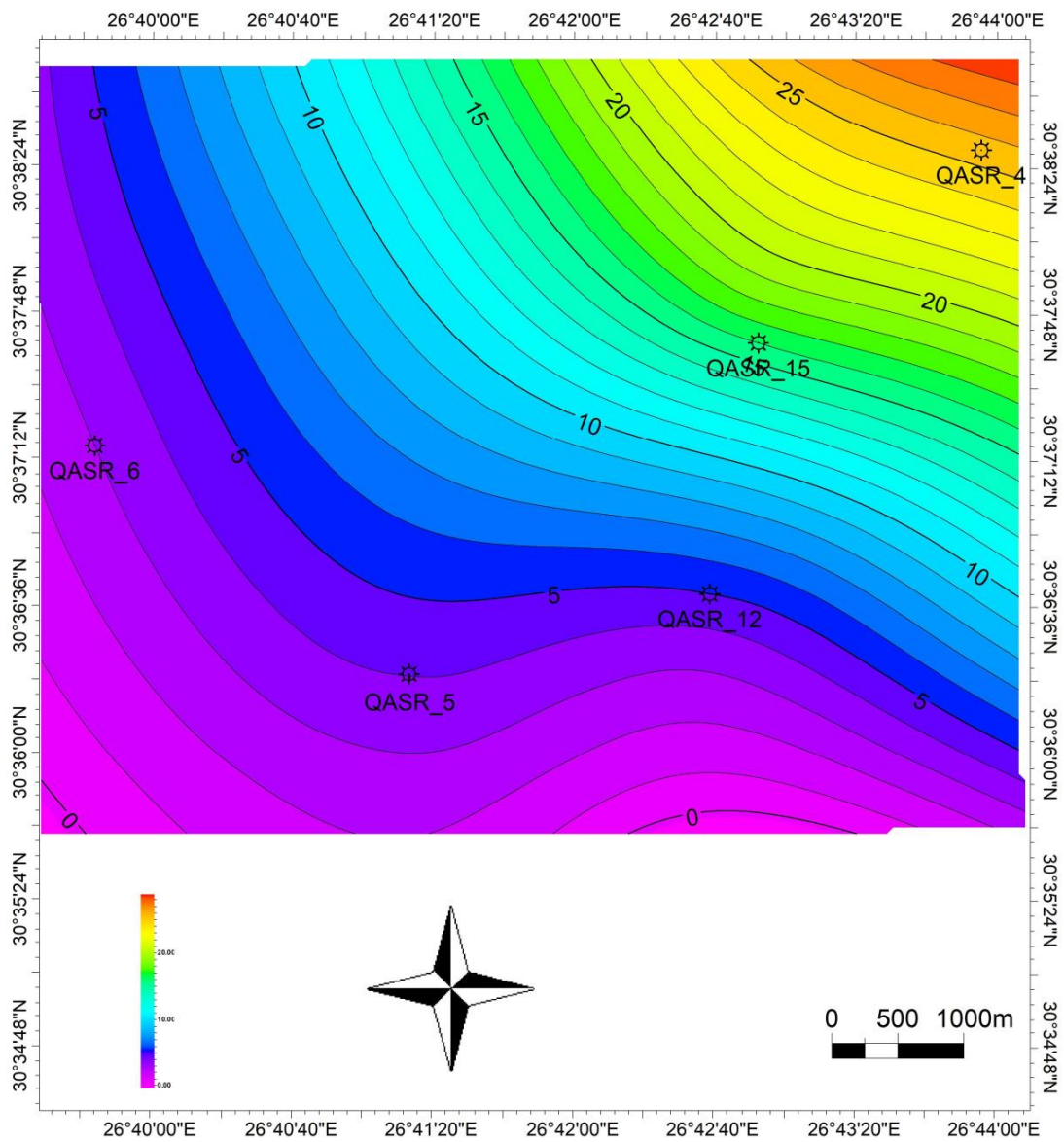


**Fig. 13: Shale content distribution map for the lower Safa Member Qasr field. This map illustrates that the shale content increases in the north and east parts and decreases gradually to the south and west part of the study area.**

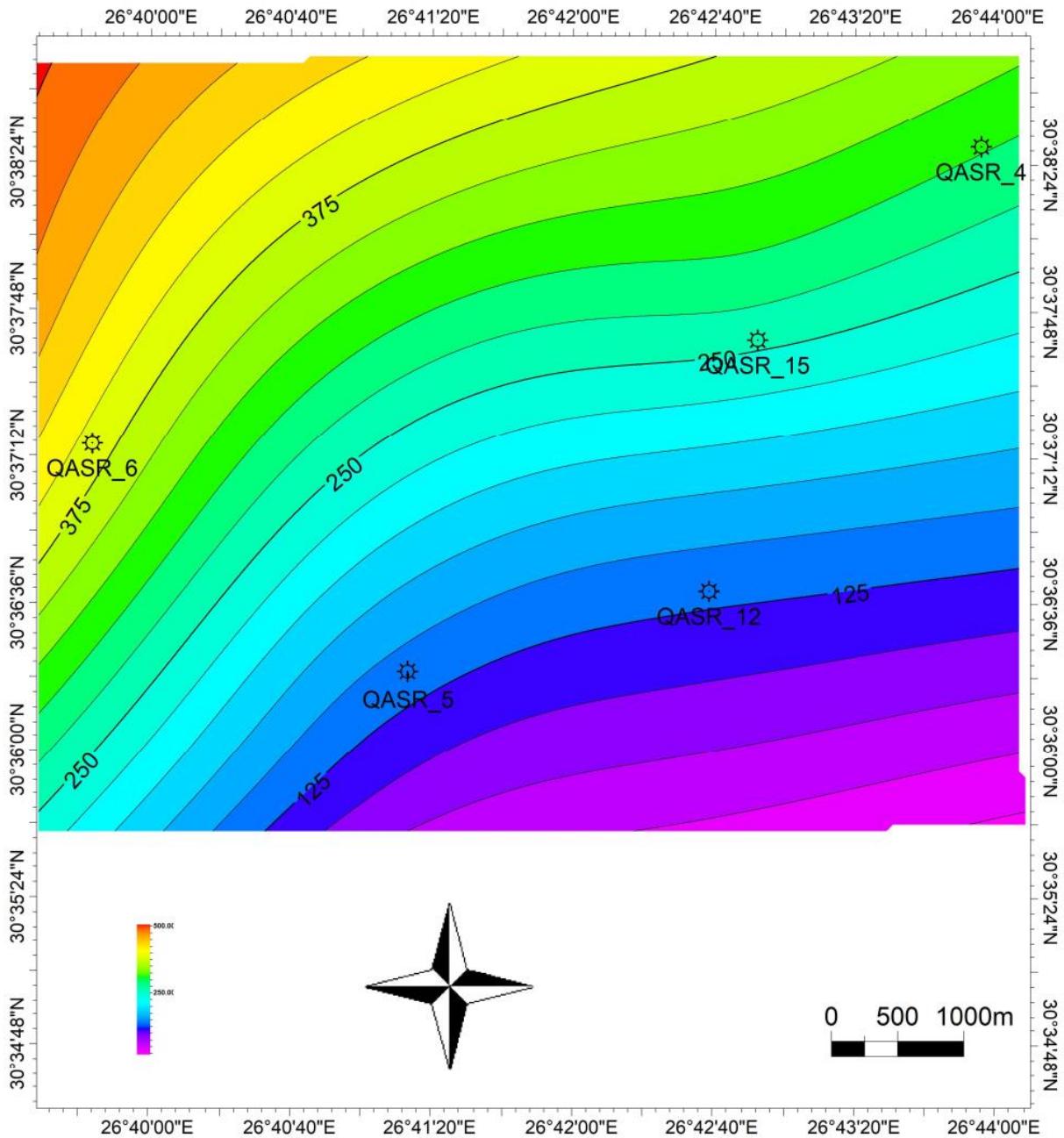


**Fig. 14: Net pay thickness map for the Lower Safa Member in Qasr field. This map illustrates that net pay increases in the central part , north and west parts of study area and decreases in the southeastern part of the study area.**

**FMI INTERPRETATION**

The sandy layers in hydrocarbon bearing section are thick sand without thin dispersed shale layers. Clays often appear as low resistivity rocks since the mineral lattice holds water molecules inside which help. an electrical current to pass through the rock easily. Pore sizes in clay rocks are very small such that hydrocarbon cannot migrate into clay porosity due to enormous capillarity of these micro pores. The structureless nature of the sandstone suggests relatively rapid deposition

which has precluded the formation of primary sedimentary structures. cross-bedding indicates deposition in high energy deposition, sand bedding, deformed bed and it was affected by conductive fracture, deformed bed, induced fracture and breakout deposition possibly occurred en-masse from sand-rich high-density turbidity currents. Minor alignment indicates that a minor tractional component of sediment transport has occurred Fig. 14.



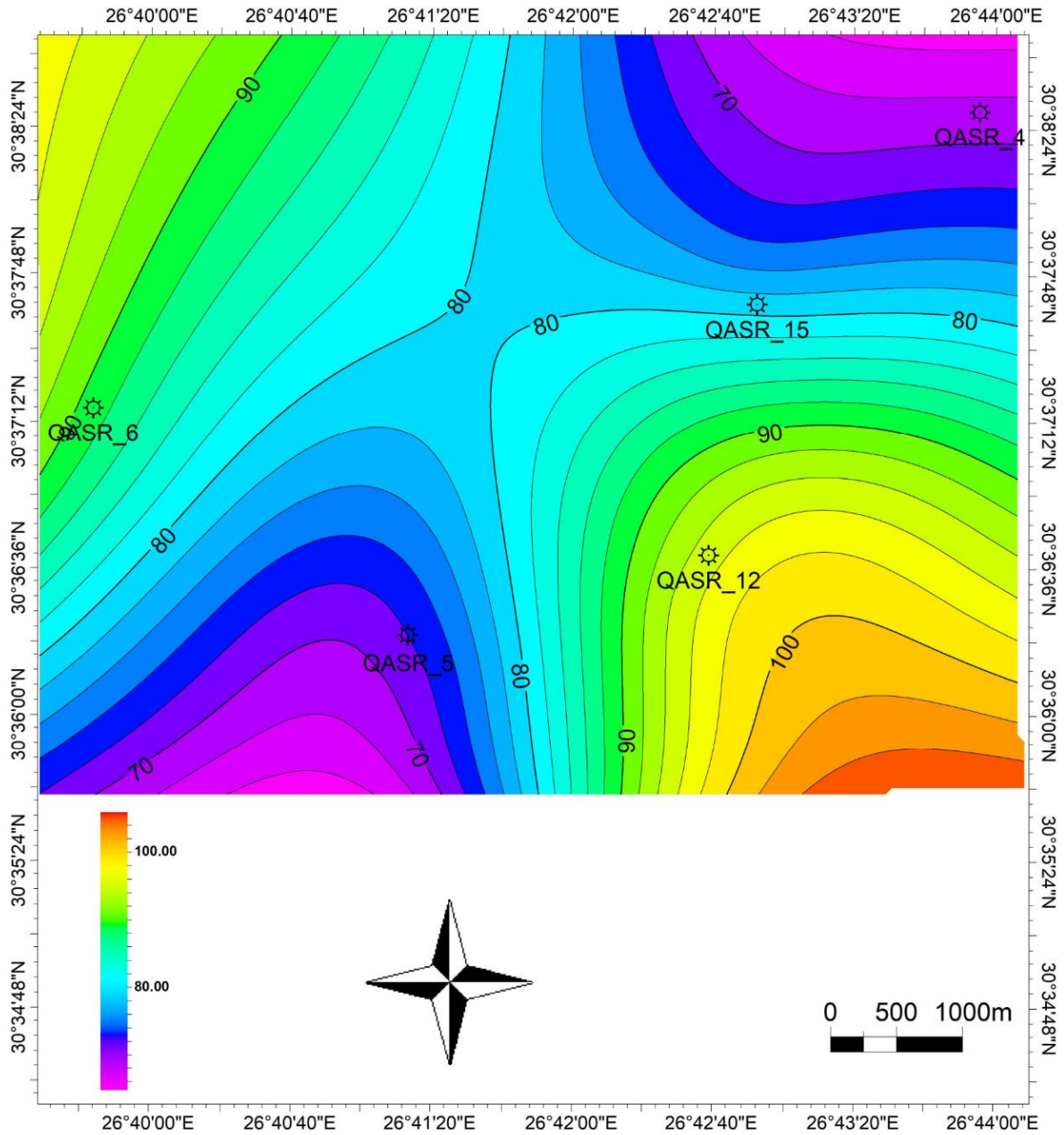


**Fig. 15: Hydrocarbon saturation map for the Lower Safa Member . This map illustrates that the hydrocarbon saturation increases in the central and northwestern parts, southeast part in the study area and decreases in the southwestern and northerneast parts of the study area.**

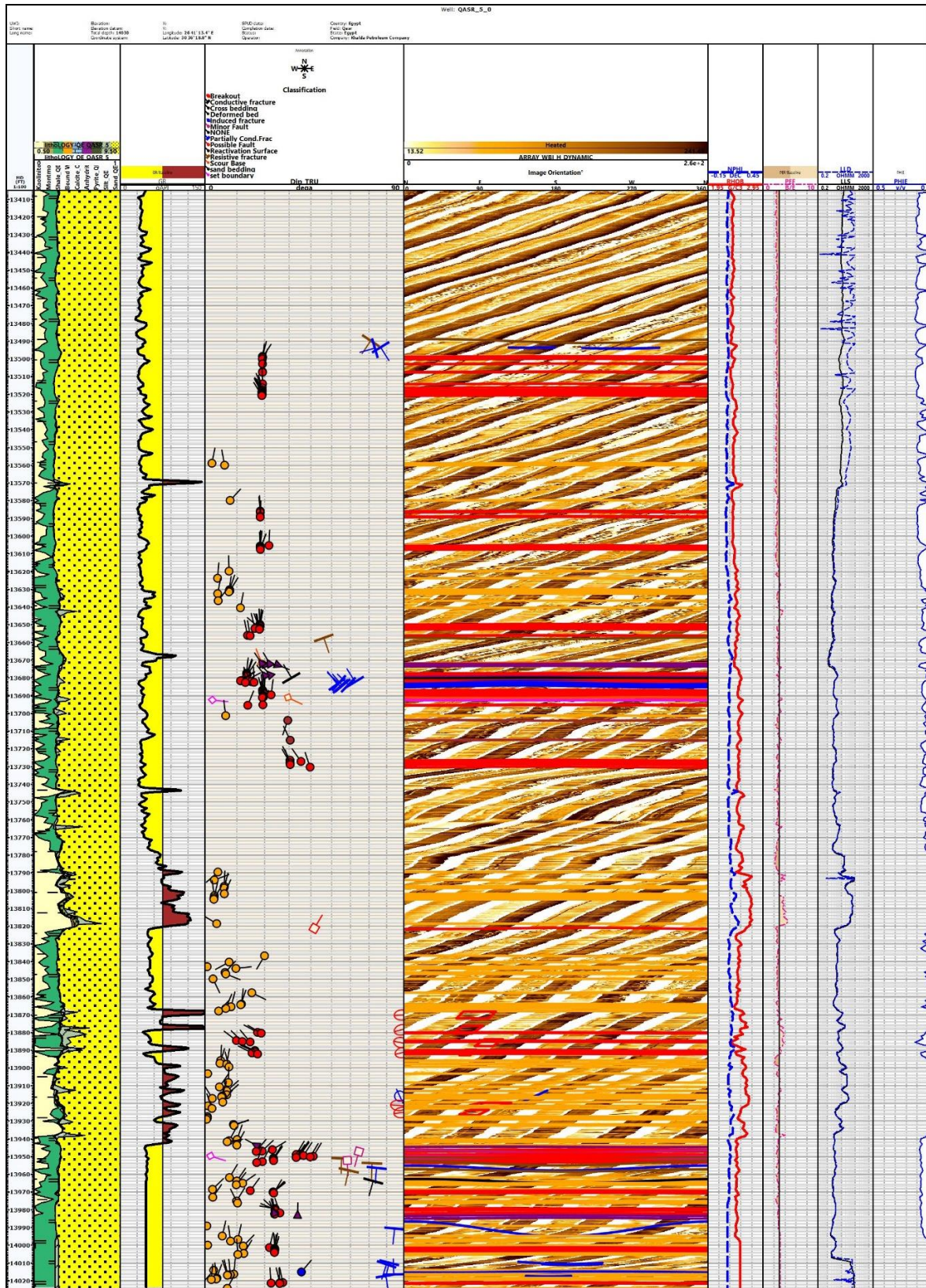


Fig. (16): FMI image log for the Lower Safa Member QASR\_4 well.

## CONCLUSIONS

The use of conventional logs alone will allow gross quantification of the hydrocarbons, lithology and pore volumes within heterolithic intervals. The comprehensive well log analysis of the Lower Safa Member in Khalda land field indicate that it is composed of sandstone intercalated with shale cemented with calcite and dolomite, whereas the sandstone thickness increases in the central and south east parts of the study area, the net pay is around 108 ft to 390 ft, The effective porosity ranges from 11.5% to 16.1%, the water saturation from 5-29%, and hydrocarbon saturation from 71-95% in study area; shale volume range from 3-16 % also the presence of dispersed shale. As a result of using petrophysical parameters distribution maps and petrophysical evaluation, the Lower Safa Member is considered as a good reservoir, which can delineate more fluids with high porosity, especially the central part of the study area that is characterized by high hydrocarbon saturation and high net pay thickness with low shale volume and high effective porosity.

**Thomas, E.C. and Stieber, S.J. (1975):** The distribution of shale in sandstones and its effect upon porosity: 16<sup>th</sup> Annual Logging Symposium, SPWLA, Paper T .

## REFERENCES

- Dolson, J.C., Shann, M.V., Matbouly SI, Hammouda H, Rashed RM (2001):** Egypt in the twenty-first century, petroleum potential in offshore trends. *GeoArabia* 6: 211-230.
- Dandekar Abhijit, Y. (2006):** Petroleum reservoir rock and fluid properties. Boca Raton, FL: CRC/Taylor & Francis.
- Egyptian General Petroleum Corporation (EGPC) (2009) :** Geologic information of the Qarun oilfield in the North Western Desert, Egypt.
- El Ayouty, M.K. (1990) :** Petroleum geology. In: Said R (ed) *The geology of Egypt*. A.A. Balkema, Rotterdam, pp 567–599.
- Schlumberger, (1972):** The essentials of log interpretation practice. Schlumberger Ltd., France, pp 45-67.
- Schlumberger, (2009):** Schlumberger Log Interpretation Charts Edition, Sugar land, Texas, USA, Schlumberger.
- Shalaby, M.R., Hakimi, M.H. and Abdullah, W.H. (2014):** Diagenesis in the Middle Jurassic Khatatba Formation sandstones in the Shoushan Basin, Northern Western Desert, Egypt. *Geol. J.* 49: 239–255
- Serra, O. (1984):** Fundamentals of well log interpretation, Elsevier, Amsterdam, 250 p
- Schon, J.H. (2011):** Physical Properties of Rocks, Vol. 8:A Workbook (Handbook of Petroleum Exploration and Production). Elsevier, Netherlands, 337-361.

